Biometals (2012) 25:165–180
DOI 10.1007/s10534-011-9494-6

Effects of dietary methylmercury on the zebrafish brain: histological, mitochondrial, and gene transcription analyses

Sébastien Cambier · Patrice Gonzalez · Nathalie Mesmer-Dudons · Daniel Brèthes · Masatake Fujimura · Jean-Paul Bourdineaud

Received: 30 April 2011 / Accepted: 7 September 2011 / Published online: 25 September 2011

Abstract The neurotoxic compound methylmercury (MeHg) is a commonly encountered pollutant in the environment, and constitutes a hazard for wildlife and human health through fish consumption. To study the neurotoxic impact of MeHg on piscivorous fish, we contaminated the model fish species *Danio rerio* for 25 and 50 days with food containing 13.5 μg/g dry weight (dw) of MeHg (0.6 μg MeHg/fish/day), an environmentally relevant dose leading to brain mercury concentrations of 30 ± 4 μg of Hg g^{-1} (dw) after 25 days of exposure and 46 ± 7 μg of Hg g^{-1} (dw) after 50 days. Brain mitochondrial respiration was not modified by exposure to MeHg, contrary to what happens in skeletal muscles. A 6-fold increase in the expression of the *sdh* gene encoding the succinate dehydrogenase Fe/S protein subunit was detected in the contaminated brain after 50 days of exposure. An up regulation of 3 genes, *atp2b3a*, *atp2b3b*, and *slc8a2b*, encoding for calcium transporters was noticed after 25 days of exposure but the *atp2b3a* and *atp2b3b* were repressed and the *slc8a2b* gene expression returned to its basal level after 50 days, suggesting a perturbation of calcium homeostasis. After 50 days, we detected the up regulation of glial fibrillary acidic protein and glutathione *S*-transferase genes (*gfap* and *gst*), along with a repression of the glutathione peroxidase gene *gpx1*. These results match well with a MeHg-induced onset of oxidative stress and inflammation. A transmission electron microscopic observation confirmed an impairment of the optical tectum integrity, with a decrease of the nucleal area in contaminated granular cells compared to control cells, and a lower density of cells in the contaminated tissue. A potential functional significance of such changes observed in optical tectum when considering wild fish contaminated in their natural habitat might be an impaired vision and therefore a lowered adaptability to their environment.

Keywords Methylmercury · Dietary exposure · Zebrafish · Bioenergetics · Brain

S. Cambier · P. Gonzalez · N. Mesmer-Dudons · J.-P. Bourdineaud (✉)
Arcachon Marine Station, UMR 5805, CNRS, Université de Bordeaux, Place du Dr Peyneau, 33120 Arcachon, France
e-mail: jp.bourdineaud@epoc.u-bordeaux1.fr

D. Brèthes
Institut de Biochimie et Génétique Cellulaires, UMR 5095, CNRS, Université de Bordeaux, 1, rue Camille Saint Saëns, 33077 Bordeaux Cedex, France

M. Fujimura
Pathology Section, Department of Basic Medical Sciences, National Institute for Minamata Disease, 4058-18 Hama, Minamata, Kumamoto 867-0008, Japan

Introduction

Methylmercury (MeHg) accumulates to appreciable levels in brain tissues of fish-eating wildlife and

humans (Clarkson et al. 2003). This metal easily goes through the blood–brain barrier using L-type amino acid transporters with, for example, the MeHg-L-cysteine complex (Aschner 1989). This accumulation of MeHg in brain leads to a loss of neurons in the calcarine cortex and granular cells of cerebellum (Oyake et al. 1966; Eto 2000). MeHg leads to neuron death in both in vitro and in vivo studies with a more significant accumulation of MeHg in astrocytes (Davis et al. 1994; Charleston et al. 1996).

We recently reported a survey of the impact of dietary MeHg on the muscle mitochondrial metabolism of a model adult fish species, the zebrafish *Danio rerio*, with food containing 13.5 μg of MeHg/g, dry weight (dw), an environmentally relevant dose. In muscle fibers, the mitochondrial respiration at both state 3, actively respiring state of mitochondria through ADP consumption, and state 4, respiring state of mitochondria when ATP synthase is inhibited, were followed. This approach showed a strong inhibition of both state 3 mitochondrial respiration and functionally isolated maximal cytochrome *c* oxidase (COX) activity after 49 days of MeHg exposure. Accordingly, we measured a dramatic decrease in the rate of ATP production (Cambier et al. 2009). Mitochondria from contaminated zebrafish muscles presented structural abnormalities under electron microscopy observation such as cristae disorganization, outer membrane bubbling and a decrease of total area (de Oliveira Ribeiro et al. 2008; Cambier et al. 2009). A gene transcription analysis was performed at the genome-wide scale in skeletal muscles of zebrafish which showed a strong impact of MeHg on 14 ribosomal protein genes, indicating a perturbation of protein synthesis. Several genes involved in mitochondrial metabolism, the electron transport chain, endoplasmic reticulum (ER) functioning, detoxification, and general stress responses were differentially regulated, suggesting an onset of oxidative stress and ER stress. Several other genes for which transcription varied with MeHg contamination could be clustered in various cellular functions, such as lipid metabolism, calcium homeostasis, iron metabolism, muscle contraction, and cell cycle regulation (Cambier et al. 2010).

An in vitro study on rat striatal synaptosomes has shown an inhibition of the mitochondrial respiration under MeHg exposures ranging from 0.5 to 2 mg/l (Dreiem et al. 2005). MeHg also increased cytosolic and mitochondrial calcium levels in striatal synaptosomes of rats as soon as 0.1 mg/l (Dreiem and Seegal 2007). This latter study showed that cytosolic calcium elevations were largely independent of extrasynaptosomal calcium and they suggest that ROS are not the cause of mitochondrial dysfunction in striatal synaptosomes after MeHg exposure but a downstream event that reflects MeHg-induced mitochondrial dysfunction due to increased mitochondrial calcium levels.

Furthermore, in vitro experiments utilizing rats synaptosomes, rats granular cells, or NG108-15 cell line have shown that one of the earliest effects of MeHg is perturbation of the homeostasis of Ca^{2+} as well as other divalent cations (Denny et al. 1993; Hare et al. 1993; Komulainen and Bondy 1987; Limke and Atchison 2002; Marty and Atchison 1997; Sarafian 1993). MeHg causes a biphasic increase in intracellular calcium concentration. The initial increase is associated with the release of Ca^{2+} from intracellular stores. This is followed by a second increase due to the entry of extracellular Ca^{2+} (Hare and Atchison 1995a, b; Limke and Atchison 2002; Limke et al. 2004a, b; Marty and Atchison 1997). Intracellular accumulation of Ca^{2+} was also observed in rats treated with dimethylmercury by injection at 5 mg/kg/day for 12 days (Mori et al. 2000). Ca^{2+} homeostasis is also critical for mitochondrial metabolism since these organelles store Ca^{2+} and release it after acute MeHg exposure (Limke et al. 2003). If Ca^{2+} concentrations become too high, mitochondrial dysfunction occurs, triggering an increase in reactive oxygen species (ROS) generation, finally leading to cellular apoptosis (Aschner et al. 2007).

Another aspect of MeHg neurotoxicity is linked to the induction of astrocyte dysfunctions such as the uptake of extracellular glutamate and glutathione synthesis (Allen et al. 2001; Aschner et al. 2000). Furthermore, MeHg toxicity could be prevented in cerebral neuron culture by using a *N*-methyl-D-aspartate receptor antagonist (Park et al. 1996). Therefore, glutamate homeostasis seems to be one of the main targets of MeHg toxicity when dealing with astrocyte dysfunction. MeHg is also known as a disruptor of GABAergic synapses. In fact, MeHg targets $GABA_A$-type receptors (a GABA-gated chloride channel) by making synapses more excitable before their complete neutralization (Atchison 2005).

In order to acquire a better understanding of MeHg neurotoxicity and possible adaptation of the central

nervous system against this metal, we checked whether the mitochondrial metabolism in brain could be as sensitive as that of skeletal muscles.

We set up a laboratory experiment in which zebrafish were contaminated for 25 and 50 days through diet, using food containing 13.5 μg Hg/g. This mercury concentration corresponds to that found in various preys of the food web in French Guiana. Indeed, extremely high mercury level of 3.82 mg/kg in Piraiba (*Brachyplatystoma filamentosum*) was observed in Teles Pires river near Alta Floresta, far upstream in the Tapajós river basin (Akagi et al. 1995), 3.92 mg Hg/kg in fish from the Madeira River, an Amazon River tribute and up to 4 mg Hg/kg in the fish species *Pellona castealneana* caught in the Jamari River, a tribute of the Tapajós river (Malm et al. 1997). These concentrations were given on a fresh weight basis and therefore correspond to dry weight concentrations of about 13–16 mg Hg/kg. In French Guiana fish, concentrations up to 14.3 mg Hg/kg (dw) could be reported in the upper part of the Petit-Saut reservoir (Durrieu et al. 2005). Therefore, while choosing such concentration, we aimed to mimic what happens when a piscivorous fish consume another polluted fish or when necrophagous fish consume the bodies and remains of dead piscivorous fish. Fish were fed each day with a food quantity representing 5% of their body weight (44 mg food/day/fish representing 0.6 μg Hg/fish/day or 3 nmol Hg/fish/day). In a previous work we have shown that, at this contamination pressure, brain accumulated 63.5 μg Hg/g after 63 days but after having selected 13 genes known to intervene during the adaptive or stress response against metal contamination, none of them displayed a differential regulation after MeHg exposure. Yet, these genes were differentially regulated in liver and skeletal muscles after contamination (Gonzalez et al. 2005).

Here we investigated the effects of such a dietary MeHg contamination on the mitochondrial bioenergetics of zebrafish brain. A transcriptional analysis was also performed on 23 selected genes involved in antioxidant defenses, Ca^{2+} transport, glutamatergic and GABAergic synapses, genes that had not been scrutinized in the former study (Gonzalez et al. 2005). The antioxidant response was investigated using the glutathione peroxidase and the glutathione *S*-transferase genes. Ten genes were used to analyze effects of MeHg on Ca^{2+} homeostasis with six of them encoding for plasma membrane Ca^{2+} ATPase (PMCA) and the four others encoding for the Na^{+}/Ca^{2+} exchanger (NCX). When considering glutamatergic synapses, six genes were analyzed, two were selected to investigate MeHg effects on both *N*-methyl-D-aspartate (NMDA) and α-amino-3-hydroxy-5-methylisoazol-4-propionate (AMPA) glutamate receptor genes, and the four others are involved in glutamate metabolism. In the case of GABAergic synapses three genes were taken into account, two that are involved in GABA metabolism and one encoding for the β subunit of $GABA_A$ receptor. A histological study was also performed to check whether MeHg contamination could result in observable damages, such as a triggering of apoptosis or a decline of cell density.

Materials and methods

MeHg exposure condition

Adult male fish (body weight: 0.88 ± 0.03 g, wet wt; standard length: 3.63 ± 0.05 cm, $n = 9$) were randomly housed in two tanks containing 100 l of chlorine-free (50 fish per tank), continuously oxygenated water. Throughout the experiment, the temperature was maintained at 24 ± 0.5°C. Fish in each tank were fed twice a day with a quantity of artificial food corresponding to 2.5% of the fish wet weight. Control fish were fed with non-contaminated food. In the exposure tank, fish were fed with MeHg-contaminated food containing 13.5 μg of Hg/g (dw), making a contamination pressure of 0.6 μg Hg/fish/day. Hg concentration in the control diet was 0.08 μg of Hg/g (dw). Thus, in this experiment, contaminated zebrafish ingested most principally the methylated form of mercury. The contaminated diet was prepared by mixing artificial fish food (Dr. Bassleer's biofish food, tropic type, granulate size M, which is manufactured by Aquarium Münster Pahlsmeier, Telgte, Germany) with an ethanolic solution of MeHg chloride (Alltech) as previously described (Gonzalez et al. 2005). This dietary exposure level is in the range of those found in various piscivorous and invertivorous fish inhabiting natural lakes or flooded reservoirs in North America, Canada, and Brazil (Wiener et al. 2003). To minimize fish contamination via the water, one-third of the water volume from each tank was changed every 2 days, and tank bottoms were cleaned every day to eliminate fish feces and food remains.

Animal tissue sampling

Fish were removed after 25 and 50 days and killed within seconds by immersion in melting ice. This is in agreement with the ethical guidelines established and used by the NIH intramural research program (http://oacu.od.nih.gov/ARAC/documents/Zebrafish.pdf). Fish were dissected on ice and brains were independently collected. For gene expression analysis, five replicates were then created by extracting mRNA from individual fish sampled at 25 and 50 days. Mitochondrial respiration measurements were performed on the whole brain of one fish (five replicates). Each brain was excised from fish and homogenized in a respiration buffer before measurement.

Hg quantification

Before mercury quantification brain from 3 fish per condition and time of exposure were harvested and dried for 48 h at 45°C. Then, total Hg concentrations in fish brains were determined by flameless atomic absorption spectrometry. Analyses were carried out automatically after thermal decomposition at 750°C under an oxygen flow (AMA 254, Prague, Czech Republic). The detection limit was 0.01 ng Hg. The validity of the analytical methods was checked during each series of measurements against three standard biological reference materials (TORT2); Hg values were consistently within the certified ranges (data not shown).

Quantitative RT-PCR

Total RNAs were extracted from about 7 mg of fresh tissue of individual brains using the Absolutely RNA RT-PCR Miniprep kit (Agilent), according to the manufacturer's instructions. For each exposure condition and each organ, five samples were analyzed individually. First-strand cDNA was synthesized from 5 µg of the total RNA using the Stratascript First-Strand Synthesis System (Agilent) according to the manufacturer's instructions. The amplification of cDNA was monitored using the DNA intercalating dye SyberGreen I. Real-time PCR reactions were performed in a LightCycler (Roche) following the manufacturer's instructions, one cycle at 95°C for 10 min and 50 amplification cycles at 95°C for 5 s, 60°C for 5 s, and 72°C for 20 s. Primer pairs used are listed in Table 1. Reaction specificity was determined for each reaction from the dissociation curve of the PCR product. This dissociation curve was obtained by following the SyberGreen fluorescence level during gradual heating of the PCR products from 60 to 95°C. Due to high sequence identity between *gstp1* and *gstp2* (90.4% sequence similarity), and conservation of regulatory elements (Timme-Laragy et al. 2009), we designed primers that amplify both of these homologs at once, henceforth referred to as *gstp*. The gene coding for the β subunit of GABA-A receptor was selected because this subunit is the one binding GABA. Among the two isoforms of the glutamate decarboxylase we chose the *gad1* gene because it is the most expressed in the brain. Selected genes related to the mitochondrial inner membrane electron transfer chain (ETC) were those encoding the subunits analyzed by Western blotting. Concerning the Ca^{2+} homeostasis, our choice was done following a previous study describing the distribution of Ca^{2+} transporter in the different tissues of the zebrafish (Liao et al. 2007). Relative quantification of each gene transcription level was normalized according to the β-actin gene transcription. Use of the *bactin1* as housekeeping gene was validated since the cycle threshold (the number of PCR cycles needed to enter in exponential phase of amplification: C_t) of this gene was almost equal for control and contaminated fish and for both exposure time. After 25 days of culture, C_t were equal to 19 ± 0.2 and 18 ± 0.4 for control and MeHg-exposed fish, respectively. After 50 days of culture, C_t were equal to 19 ± 0.2 and 18 ± 0.3 for control and MeHg-exposed fish, respectively. Since the same quantity of total RNA was used for each cDNA synthesis, this makes for the *bactin1* gene a relative expression of 1 ± 0.14, 2 ± 0.42, and 2 ± 0.56 for control and MeHg-exposed fish after 25 and 50 days, respectively. These differences were not statistically significant allowing the relative quantification of each gene expression level to be normalized according to the β-actin gene expression.

Brain preparation for respiration measurements

A single brain was put in 1.5 ml conical tube containing 70 µl of respiratory buffer (15 mM Tris pH 7.4, 75 mM saccharose, 0.1 mM EDTA, 5 mM KCl, 5 mM phosphoric acid, 225 mM mannitol) and 2 mg/ml of bovine serum albumin (BSA). Tubes were

Table 1 Accession numbers and specific primer pairs matching with *D. rerio* genes used for quantitative RT-PCR

Function	Gene	Accession number	Primer (5′-3′)
NMDA receptor	*grin1b*	NM_001144131	CATGAGAACGGCTTCATGG[a]
			GCCAGCTGCATTTGCTTCC[b]
AMPA receptor	*gria2b*	NM_131895	GTGGAGAGGATGGTGTC[a]
			GTGGCGATGCCGTAGCCT[b]
Glutaminase	*glsa*	NM_001045044	AGGCCATGCTGAGGTTG[a]
			CTGCCGTCTCTTTTTCGCT[b]
Glutamate dehydrogenase	*glud1a*	NM_212576	GCTTTGGTAATGTGGGTCTG[a]
			GCAGGGATCTGGATATCACAC[b]
Glutamate decarboxylase	*gad1b*	NM_194419	GACGTGACCTACGACACCG[a]
			GCTGGCCCTCAAAGACC[b]
Glutamine synthase	*glula*	NM_181559	GTGGGAGTTCCAGGTTGGC[a]
			GCATTGTCCAGGCCTCCTT[b]
GABA transporter	*zgc:103663*	NM_001007362	ATGCTGTTTATCCTGTTCATCCG[a]
			TGTTGAAGGGGTTGTAGCTCC[b]
GABA transaminase	*abat*	NM_201498	GCGTTCAGGCAAAGCTCT[a]
			GCAGGACGGAAACGGAT[b]
GABA receptor β subunit	*LOC566514*	XM_689786	TCACAATGACAACCATCAACA[a]
			CACTCCGGAGCTGTCAAAGG[b]
Glial fibrillary acidic protein	*gfap*	NM_131373	AGTACCAGGACCTGCTCAA[a]
			ACAGTTCGCACAACTATGCT[b]
Glutathione peroxydase 1a	*gpx1a*	NM_001007281	CACCCTCTGTTTGCGTTCC[a]
			CTCTTTAATATCAGCATCAAT[b]
Glutathione *S*-transferase	*gstp*	AF285098	CGGATTCCTGGTTGGCG[a]
			TGCCATTGATGGGCAGTTT[b]
Porin	*vdac2*	NM_199585	CTATCCACGGCGCTGC[a]
			GGCCAGATTCACCGCT[b]
β-actin	*bactin1*	NM_131031	AAGTGCGACGTGGACA[a]
			GTTTAGGTTGGTCGTTCGTTTGA[b]
Plasma membrane Ca^{2+}-ATPase			
PMCA 1a	*atp2b1a*	NM_001044757	TTCCGCAGCTCGCTGT[a]
			GGAGGTGTAGGGGTCGC[b]
PMCA 1b	*atp2b1b*	NM_001135631	GTGGTGCAGGGGTCTCA[a]
			GCGTTTGGTGGGTGCG[b]
PMCA 2	*atp2b2*	NM_001123238	ACGTGTCGTGAACGCA[a]
			CCGGCTGACTGGAGTTT[b]
PMCA 3a	*atp2b3a*	NM_001002472	ACCAAGCTGTGAGAGAGCA[a]
			GCCCTAAAAGCACGAGCC[b]
PMCA 3b	*atp2b3b*	NM_001128242	GGCCTTAACCGTATCCAGACT[a]
			ACGCTTTCACTACCCGC[b]
PMCA 4	*atp2b4*	NM_001077467	AGGGAGACAACGCTGC[a]
			CTCCTGCTCAATGCGGC[b]
Na^+/Ca^{2+} exchanger			
NCX 1b	*slc8a1b*	NM_001039144	AGTGGCAGCGATACAGG[a]
			TGAGCACCGCTACACAG[b]

Table 1 continued

Function	Gene	Accession number	Primer (5′-3′)
NCX 2a	*slc8a2a*	NM_001123296	TGTTTGTTGCTTTGGGAACCT[a]
			CAAGCGAACCGGGGTC[b]
NCX 2b	*slc8a2b*	NM_001123284	CTGGGTATCGGAGTGGC[a]
			GTGTAGTGAGCAGTCGGG[b]
NCX 4a	*slc8a4a*	NM_001089419	ATACGCCGATGCGTCC[a]
			CAGTAGTGTCACAACACATACCAG[b]
Electron transport chain complex			
Complex V	*atp5a1*	NM_001077355	GGCCTACCCCGGTGAC[a]
			CGGGACGGATACCCTTGT[b]
Complex V	*atp5f1*	NM_001005960	GTGTGACAGGGCCTTATATGC[a]
			CTGAGCCTTTGCTATTTTATCCGC[b]
Complex IV	*cox4i1*	NM_214701	AGAGTGGAAATCTGTGGTTGC[a]
			CCAAGCGTTGTTTTCATAGTCCC[b]
Complex IV	*cox1*	NC_002333 (6425–7975)	GGAATACCACGACGGTACTCT[a]
			AGGGCAGCCGTGTAAT[b]
Complex III	*mt-cytb*	NC_002333 (15308–16448)	CGCCATTCTACGATCTATCCC[a]
			GGTGTTCTACTGGTATCCCTCC[b]
Complex II	*sdhb*	NM_001098740	GGACAGCACACTGACCTT[a]
			GTTGCTCATGTCGGGCAC[b]
Complex I	*ndufs3*	NM_001017755	AGACGCATCTTGACAGATTATGG[a]
			CCCCCGGTATGCAGGA[b]

grin1b Ionotropic *N*-methyl-D-aspartate glutamate receptor 1b; *gria2b* ionotropic AMPA glutamate receptor 2b; *glsa* glutaminase like; *glud1a* glutamate dehydrogenase 1a; *gad1* glutamate decarboxylase 1; *glula* glutamate-ammonia ligase (glutamine synthase) a; *zgc:103663* solute carrier family 6 member 1 (GABA neurotransmitter transporter); *abat* 4-aminobutyrate aminotransferase; *LOC566514* similar to gamma-aminobutyric acid receptor beta subunit; *gfap* glial fibrillary acidic protein; *gpx1a* glutathione peroxidase 1a; *gstp* glutathione *S*-transferase pi; *vdac2* voltage dependent anion channel; *bactin1* beta actin 1; *atp2b* Ca^{2+} transporting plasma membrane ATPase; *slc8a* solute carrier family 8 (sodium/calcium exchanger); *atp5a1* ATP synthase subunit a, mitochondrial complex F1; *atp5f1* ATP synthase subunit b, mitochondrial complex F0; *cox4i1* COX subunit 4 isoform 1; *cox1* COX subunit 1; *mt-cytb* cytochrome *b*, mitochondrial; *sdhb* succinate dehydrogenase subunit b, protein Fe/S; *ndufs3* NADH dehydrogenase (ubiquinone oxidase) Fe–S protein 3

GenBank accession no. NC_002333 correspond to the mitochondrial genome; numbers between parentheses indicate the location within the mitochondrial genome

[a] Upstream primer

[b] Reverse primer

weighed before and after brain addition in order to determine each brain mass. Brains were gently homogenized by 13 strokes with a conical plastic pestle, and the homogenates were immediately used for respiration measurements.

Mitochondrial respiration measurements

Mitochondrial oxygen consumption was monitored polarographically at 30°C using a Clark oxygen electrode connected to an OXM 200 oxymeter (Heito, Paris, France) in a 1 ml thermostatically controlled chamber. The oxygraph cuvette contained the homogenate of one brain (6–10 mg) in 1 ml of respiratory solution with the respiratory substrates (10 mM pyruvate and 10 mM malate). The mitochondrial respiration measurements were performed on five individual brains at 25 and 50 days for control and MeHg-contaminated fish. State 3 was obtained by the addition of 2 mM ADP whereas state 4 was subsequently reached by using a combination of atractyloside (1 mM final concentration) and oligomycin (2 μg/ml final concentration). The respiratory control ratio (RCR) is defined as the ratio of state 3 to state 4 respiratory rates. Uncoupled respiration

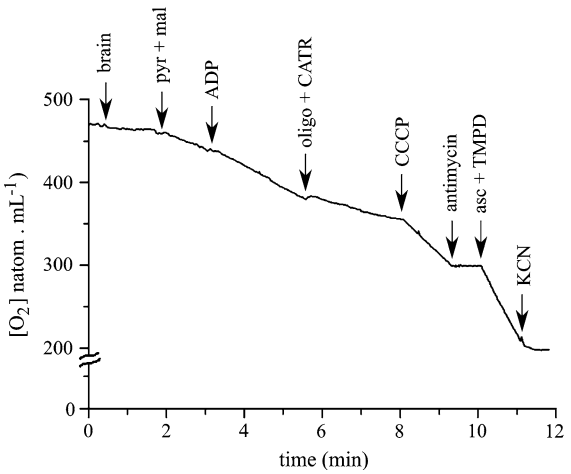

Fig. 1 Kinetic time-point experiment of mitochondrial respiration given by a single fish brain homogenate. All reagents, substrates and inhibitors addition are described in "Materials and methods" section. *pyr + mal* Addition of the carbon substrates pyruvate and malate; *ADP* addition of ADP to trigger the respiratory state 3; *oligo + ATR* addition of oligomycin and atractyloside to inhibits the functioning of ATP synthase and trigger the respiratory state 4; *CCCP* addition of carbonyl cyanide *m*-chlorophenylhydrazone, a respiration uncoupler; *asc + TMPD* addition of ascorbate and tetramethyl-*p*-phenylenediamine as an electron donor system to cytochrome *c*; *KCN* addition of potassium cyanide

rates were measured after the addition of 2 μM of carbonyl cyanide *m*-chlorophenylhydrazone (CCCP). COX or complex IV activity was monitored by specifically inhibiting the first complexes of the respiratory chain with 2 μg/ml antimycin, and using 12.5 mM ascorbate and 1.5 mM tetramethyl-*p*-phenylenediamine (TMPD) as an electron donor system. The respiratory rate was monitored with the polarographic method described above.

A typical time-course oxygen consumption plot obtained with one control fish brain is given on Fig. 1. This indicates that the enzymatic respiratory material contained in one single brain is sufficient to allow a complete mitochondrial respiratory experiment, and to accurately measure oxygen consumption rates.

Hematoxylin and eosin staining and NeuN immunohistochemical staining of brain sections

Histological analyses were performed as described previously (Fujimura et al. 2009). In brief, after 50 days of exposure five brains from five different fish per condition were excised, fixed with 4% paraformaldehyde (Wako Pure Chemical Industries Ltd, Osaka, Japan) in phosphate-buffered saline (Sigma-Aldrich, St Louis, USA), and embedded in paraffin-wax; further, 5-μm coronal sections were cut using a microtome. For routine light microscopy, the paraffin sections were stained with hematoxylin and eosin. Immunohistochemical analyses for neuronal nuclei were performed using a mouse anti-neuronal nuclei monoclonal antibody (MAB377, clone A60, Chemicon, Millipore corporation) and the Vectastain Elite ABC Kit based on peroxidase detection (Vector Laboratories, Burlingame, USA). NeuN antibody specifically recognizes the DNA-binding, neuron-specific protein NeuN, which is present in most neuronal cell types. The sections were mounted with Crystal Mount (Biomeda, Foster City, USA).

Preparation of tissues for transmission electron microscopy analysis

After 50 days of exposure, harvested brains from five control and four MeHg-contaminated fish were immediately immersed in a fixing solution (3% glutaraldehyde buffered with 0.1 mmol/l sodium cacodylate solution, pH 7.4; osmolarity 600 mosmol/l) for 12 h at 4°C then rinsed in a cacodylate buffer (0.1 mmol/l, 2% NaCl). After dehydration, brains were embedded in Araldite epoxy in order to prepare different types of sections using an automatic ultra-microtome (Reichert). For electronic microscopy, ultrafine sections (500–700 Å) were placed on grids and further observed under a Philips CM10 electron microscope.

Image and statistical analysis

Image acquisition and processing were performed with Meta Imaging (MetaView serie 5.0 and MetaMorph serie 5.0, Universal Imaging Corporation, USA). To determine the size of the nucleus, a graphic pencil was used to delimit area of interest. The numbering of cells in the optical tectum was performed using the ImageJ 1.43 software (National Institutes of Health, United States of America). All the computations were carried out with Statistica software (StatSoft, USA). Significant differences in the distribution of nucleus surfaces between control and exposed brain were determined using the Mann–Whitney *U*-test ($P < 0.05$).

Inter-individual variability for each experimental condition was defined by mean ± SEM ($n = 5$). Significant differences between respiratory rates, COX activity and gene transcription levels in brains were determined using the nonparametric Mann–Whitney U-test ($P < 0.05$).

Results

Mercury quantification

After 25 days of exposure to 3 nmol of MeHg/fish/day (0.6 μg of MeHg/fish/day), fish brains accumulated a high level of mercury, 30.2 ± 4.2 μg of Hg g^{-1} (dw), compared to control brains, 0.19 ± 0.03 μg of Hg g^{-1} (dw). After 50 days of exposure the mercury level increased to 46.2 ± 7.3 μg of Hg g^{-1} (dw), whereas in the control brains the Hg remained at a very low level, 0.96 ± 0.08 μg of Hg g^{-1} (dw). This illustrates the high efficiency of MeHg to cross the blood–brain barrier.

Brain mitochondrial respiration

The mitochondrial respiration was directly measured on brain homogenates from control and MeHg-contaminated fish after 25 and 50 days using pyruvate and malate as substrates. It appeared that state 3 (obtained after addition of ADP) and state 4 (no ATP synthesis, basal respiration) of the mitochondrial respiration were not significantly changed (Fig. 2a). Calculation of the RCR, which is the ratio of the respiratory rate at state 3 over that at state 4, did not reveal any significant effect of MeHg contamination on the coupling of mitochondrial respiration with ATP synthesis (Fig. 2b). Uncoupled respiration measured in presence of CCCP presented no difference between control and contaminated fish brains (Fig. 2c). When COX was fed with electrons directly through ascorbate and TMPD in the presence of rotenone and antimycin, thereby bypassing the rest of the ETC, no difference was observed between control and contaminated fish brains (Fig. 2d).

Gene transcription levels

The transcription pattern of genes encoding for subunits of the electron transport chain was assayed. Gene transcriptions of ATP synthase subunits α and β did not change under MeHg contamination. The succinate dehydrogenase Fe/S subunit gene presented a 6-fold significantly increased transcription after 50 days of contamination (Table 2). Due to the high measure of variability of the other genes studied, the mean differential transcriptions between control and contaminated brains were not statistically significant despite an induction or repression factor of greater than 2.

Transcription of different genes involved in the metabolisms of GABAergic and glutamatergic synapses were studied after 25 and 50 days of exposure. Genes encoding the β subunit of GABA receptor (*LOC566514*) and glutamate receptors (NMDA-type, *grin1b*, and AMPA-type, *gria2b*) showed no significant differential transcription between control and contaminated fish after 25 and 50 days of exposure (Table 3). The transcription of genes encoding for proteins involved in glutamate and GABA metabolic pathways revealed a 3.5-fold up-regulation of a gene (*abat*) encoding for GABA transaminase, a GABA degradation enzyme, after 50 days of exposure (Table 3).

After 50 days of exposure, transcription levels of *gst* and *gfap* genes were up-regulated 2.5- and 8-fold, respectively, whereas the transcription level of *gpx1* was repressed 2.3-fold. *vdac2* gene transcription was up-regulated 2.6-times after 25 days of exposure with a return to basal level after 50 days (Table 3).

Among ten selected genes encoding for Ca^{2+} transporters, an increased transcription was observed after 25 days of exposure for three genes: *atp2b3a*, *atp2b3b*, and *slc8a2b*. After 50 days, the genetic response shifted towards down-regulation for both *atp2b3a* and *atp2b3b* genes, and a return of *slc8a2b* transcription to levels similar to control levels.

Analysis of brain ultrastructure by microscopy

After 50 days of exposure, brains were collected and sections of the granular cell layer from the optic tectum were observed by microscopy. By performing hematoxylin and eosin staining and immunohistochemical analyses with anti-NeuN antibody, we could not assessed at this scale any neuropathological changes in samples obtained from MeHg-contaminated zebrafish compared to control fish (Fig. 3).

However, the histological analysis performed with transmission electron microscopy, evidenced a

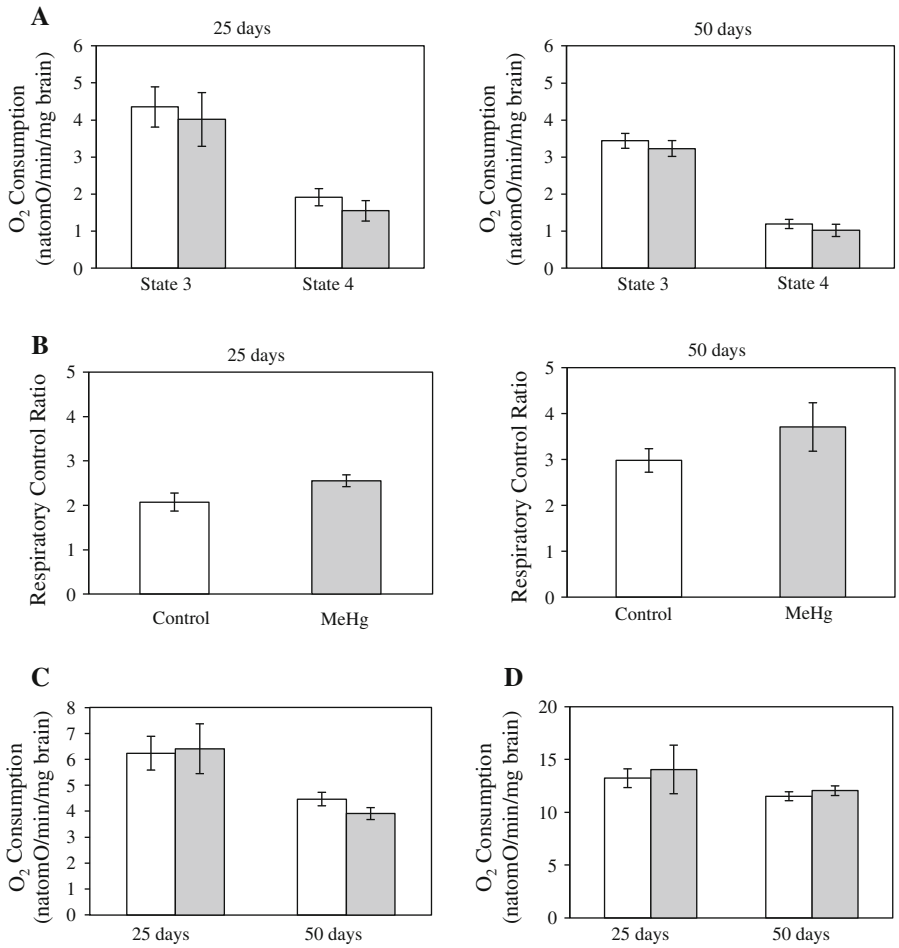

Fig. 2 MeHg dietary contamination (0.6 μg Hg day^{-1} $fish^{-1}$) had no detectable effect on mitochondrial respiratory activity. **a** Oxygen consumption measured in brain homogenate from control and MeHg-contaminated fish after 25 and 50 days. Mitochondrial respiration was stimulated by addition of pyruvate and malate. **b** Coupling between state 3 and state 4. Respiratory control ratio: ratio of oxygen consumption rates as observed at state 3 over that at state 4. *Open bars* control fish, and *grey bars* contaminated fish (mean ± SEM, $n = 5$). **c** Uncoupled respiration measured in presence of CCCP. *Open bars* control fish, and *grey bars* contaminated fish (mean ± SEM, $n = 5$). **d** COX activity in the zebrafish brain. Electrons were directly supplied to complex IV by the addition of ascorbate and TMPD in the presence of complex I and II inhibitors, rotenone and antimycin, respectively. *Open bars* control fish, and *grey bars* contaminated fish (mean ± SEM, $n = 5$)

decrease of the nucleal area in contaminated granular cells compared to control cells, and a lower density of cells in the contaminated tissue, evidenced by a decreased number of nuclei per surface unit (Fig. 4). In order to quantify the decrease of nucleal area and cell density, a statistical analysis of images from the microscopic photography was performed. Analysis was performed on 1101 and 482 nuclei from control and contaminated fish, respectively, and confirmed the size decrease of nuclei in granular cells from contaminated fish compared to their control counterparts (Fig. 4). Indeed, in contaminated granular cells layer 94% of nuclei possessed a surface of less than 11 μm^2 compared to only 66% in control ($P < 0.001$). The measured cell densities were 4.2 ± 0.1 nucleuses per 100 μm^2 and 3.9 ± 0.1 nucleuses per 100 μm^2 in control and contaminated tissues ($P < 0.05$), respectively. However, microscopic analysis did not reveal any alteration of mitochondrial shape.

Table 2 Differential gene transcription of respiratory chain complexes observed in zebrafish brain after dietary contamination with MeHg (0.6 μg Hg day^{-1} $fish^{-1}$)

Gene	Control 25 days	Contaminated 25 days	Response factor[a]	Control 50 days	Contaminated 50 days	Response factor[a]
ndufs3	$(3.7 \pm 0.3) \times 10^{-5}$	$(2 \pm 1) \times 10^{-5}$	0.5	$(8 \pm 3) \times 10^{-6}$	$(2 \pm 1) \times 10^{-6}$	0.25
sdh	0.13 ± 0.04	0.11 ± 0.02	0.8	0.03 ± 0.001	0.18 ± 0.04	6**
cytb	636 ± 192	250 ± 113	0.4	63 ± 8	65 ± 12	1
cox 4	8 ± 1	4.6 ± 1	0.6	11 ± 2	33 ± 14	3
cox 1	19 ± 4	16 ± 3	0.8	3.8 ± 1	3.6 ± 0.5	0.9
atp5a1	1.2 ± 0.5	0.9 ± 0.2	0.75	0.5 ± 0.05	0.7 ± 0.05	1.4
atp5f1	6.2 ± 1	12 ± 3	2	1.6 ± 0.3	1.3 ± 0.2	0.8

Results are given relative to the *bactin1* gene transcription level (mean ± SEM; $n = 4$ for 25 days and $n = 5$ for 50 days)

[a] Response factor is the ratio between the relative transcription in contaminated fish tissue over that in control fish tissue

** Significant differential transcription as compared to control fish (Mann–Whitney U test, $P < 0.05$)

Discussion

We have already reported several mitochondrial impairments in zebrafish skeletal muscle fibers after dietary MeHg exposure at the same contamination pressure, such as mitochondrial ultrastructural disorganization, inhibition of state 3 mitochondrial respiration and inhibition of COX (de Oliveira Ribeiro et al. 2008; Cambier et al. 2009). But surprisingly, in the present study no impact on the brain was observed at the mitochondrial ultrastructural level, or on mitochondrial respiratory activity after 25 and 50 days of MeHg exposure although brain accumulated 50% more mercury than muscles (46 against 32 μg/g, respectively). A nonetheless important point to underline is the complexity of brain. For example, in MeHg-treated rats at a dose of 10 mg/kg/day, a decrease in oxygen consumption at both state 3 and 4 and an increase in ROS generation were found in mitochondria prepared from the cerebellum but not from the cerebrum (Mori et al. 2007). So, the complexity of the central nervous system could lead to obscure possible impacts of MeHg on mitochondrial activity since analysis were performed on the whole brain.

In the brain of the Atlantic cod treated with 2 mg MeHg/kg, the levels of F-type H^+-transporting ATPase α subunit, cytochrome *c1*, and NADH dehydrogenase Fe–S protein were increased but this proteomic approach could not give clues about the impact of MeHg on the mitochondrial respiratory function (Berg et al. 2010). In the present study we found an increase of the complex II Fe/S subunit gene expression after 50 days. This is reminiscent of the observed inhibition of succinate dehydrogenase in rat skeletal muscles after 12 days of oral MeHg contamination (5 mg MeHg kg^{-1} day^{-1}) (Usuki et al. 1998). In addition, in cerebellar mitochondria from MeHg-treated rats (10 mg MeHg/kg/day for 5 days), a decrease in oxygen consumption and an increase in ROS generation were noticed. Succinate, used as a respiratory substrate, led to an augmentation of ROS generation, suggesting that MeHg might affect the complex II–III mediated pathway in the ETC in cerebellar mitochondria (Mori et al. 2007). Thus, among ETC complexes, complex II appears to be highly sensitive to MeHg toxicity, which may be caused by the interaction between MeHg and thiol groups in this complex.

After 50 days of dietary MeHg-exposure, the gene *gpx1* was down-regulated whereas *gst* gene transcription was up-regulated in the zebrafish brain. The observed repression of the gene *gpx1* was in keeping with results obtained from analysis of the salmon brain (*Salmo salar*) where a lipid peroxidation was induced after chronic MeHg exposure, correlated with a decrease in glutathione peroxidase activity (Berntssen et al. 2003). This down-regulation of the *gpx1* gene was also observed in mouse brain after exposure to 40 mg MeHg/l in drinking water for 21 days, and in cultured human neuroblastoma SH-SY5Y cells (Franco et al. 2009). And it has just been shown that MeHg-induced selenium deficiency leads to failure of the recoding of a UGA codon for selenocysteine and results in degradation of the major antioxidant

Table 3 Differential gene transcriptions observed in zebrafish brain after dietary contamination with MeHg (0.6 μg Hg day^{-1} $fish^{-1}$)

Gene	Control 25 days	Contaminated 25 days	Response factor[a]	Control 50 days	Contaminated 50 days	Response factor[a]
Glutamate metabolism						
grin1b	0.03 ± 0.01	0.04 ± 0.01	–	0.05 ± 0.01	0.05 ± 0.01	–
gria2b	0.14 ± 0.06	0.1 ± 0.02	–	0.17 ± 0.05	0.22 ± 0.04	–
glsa	0.04 ± 0.01	0.02 ± 0.01	–	0.03 ± 0.01	0.05 ± 0.02	–
glud1a	0.06 ± 0.03	0.03 ± 0.01	–	0.026 ± 0.002	0.029 ± 0.006	–
gad1b	0.15 ± 0.04	0.21 ± 0.04	–	0.23 ± 0.04	0.29 ± 0.05	–
glula	2 ± 1	2.3 ± 0.3	–	1.9 ± 0.3	3 ± 1	–
GABA metabolism						
zgc:103663	0.05 ± 0.02	0.1 ± 0.03	–	0.14 ± 0.03	0.18 ± 0.02	–
abat	0.06 ± 0.02	0.08 ± 0.01	–	0.08 ± 0.01	0.27 ± 0.06	3.5
LOC566514	0.007 ± 0.002	0.01 ± 0.003	–	0.01 ± 0.001	0.009 ± 0.001	–
Oxidative stress						
gfap	0.02 ± 0.003	0.02 ± 0.01	–	0.011 ± 0.003	0.09 ± 0.03	8
gpx1	0.05 ± 0.02	0.05 ± 0.01	–	0.09 ± 0.02	0.04 ± 0.01	1/2.3
gst	0.08 ± 0.03	0.09 ± 0.05	–	0.04 ± 0.02	0.1 ± 0.02	2.5
vdac2	0.05 ± 0.01	0.12 ± 0.02	2.6	0.5 ± 0.1	0.8 ± 0.2	–
Calcium transporters						
atp2b1a	0.11 ± 0.04	0.12 ± 0.06	–	0.35 ± 0.12	0.11 ± 0.02	–
atp2b1b	0.67 ± 0.02	0.69 ± 0.04	–	0.43 ± 0.22	0.2 ± 0.1	–
atp2b2	$(1 \pm 1) \times 10^{-5}$	$(0.9 \pm 0.4) \times 10^{-5}$	–	$(100 \pm 100) \times 10^{-5}$	$(3 \pm 2) \times 10^{-5}$	–
atp2b3a	0.3 ± 0.1	1.6 ± 0.8	5	3.6 ± 0.7	1.2 ± 0.6	1/3
atp2b3b	0.4 ± 0.2	1.8 ± 0.9	4.2	4.7 ± 1	0.9 ± 0.2	1/5
atp2b4	$(30 \pm 20) \times 10^{-4}$	$(0.3 \pm 0.2) \times 10^{-4}$	–	$(3{,}200 \pm 3{,}200) \times 10^{-4}$	$(9 \pm 4) \times 10^{-4}$	–
slc8a1b	0.006 ± 0.003	0.007 ± 0.004	–	0.01 ± 0.01	0.002 ± 0.001	–
slc8a2a	0.0006 ± 0.0002	0.0008 ± 0.0004	–	0.002 ± 0.001	0.002 ± 0.001	–
slc8a2b	0.25 ± 0.08	1.25 ± 0.63	4.7	1.7 ± 0.5	1 ± 0.3	–
slc8a4a	$(20 \pm 10) \times 10^{-5}$	$(3 \pm 2) \times 10^{-5}$	–	$(50 \pm 40) \times 10^{-5}$	$(1 \pm 0.4) \times 10^{-5}$	–

Results are given relative to the *b-actin* gene transcription level (mean ± SEM; $n = 5$ for 25 days for 50 days)

[a] Response factor is the ratio between the relative transcription in contaminated fish tissue over that in control fish tissue. The indicated response factors were those with significant differential transcription level compared to control fish (Mann–Whitney U test, $P < 0.05$)

–, Gene featuring no significant differential transcription

selenoenzyme glutathione peroxidase 1 (GPx1) mRNA by nonsense-mediated mRNA decay (Usuki et al. 2010). Thus, the *gpx1* gene down-regulation during MeHg exposure is the perfect signature of the onset of an oxidative stress, which is confirmed by the 2.5-fold up-regulation of glutathione *S*-transferase *gst* gene. The latter enzyme is considered as a biomarker for assessing the environmental impact of xenobiotics that generate oxidative stress (Livingstone 1998).

At 50 days of exposure, *gfap* transcription was up regulated in the contaminated brain indicating the onset of neurotoxic events. Indeed, induction of *gfap* is

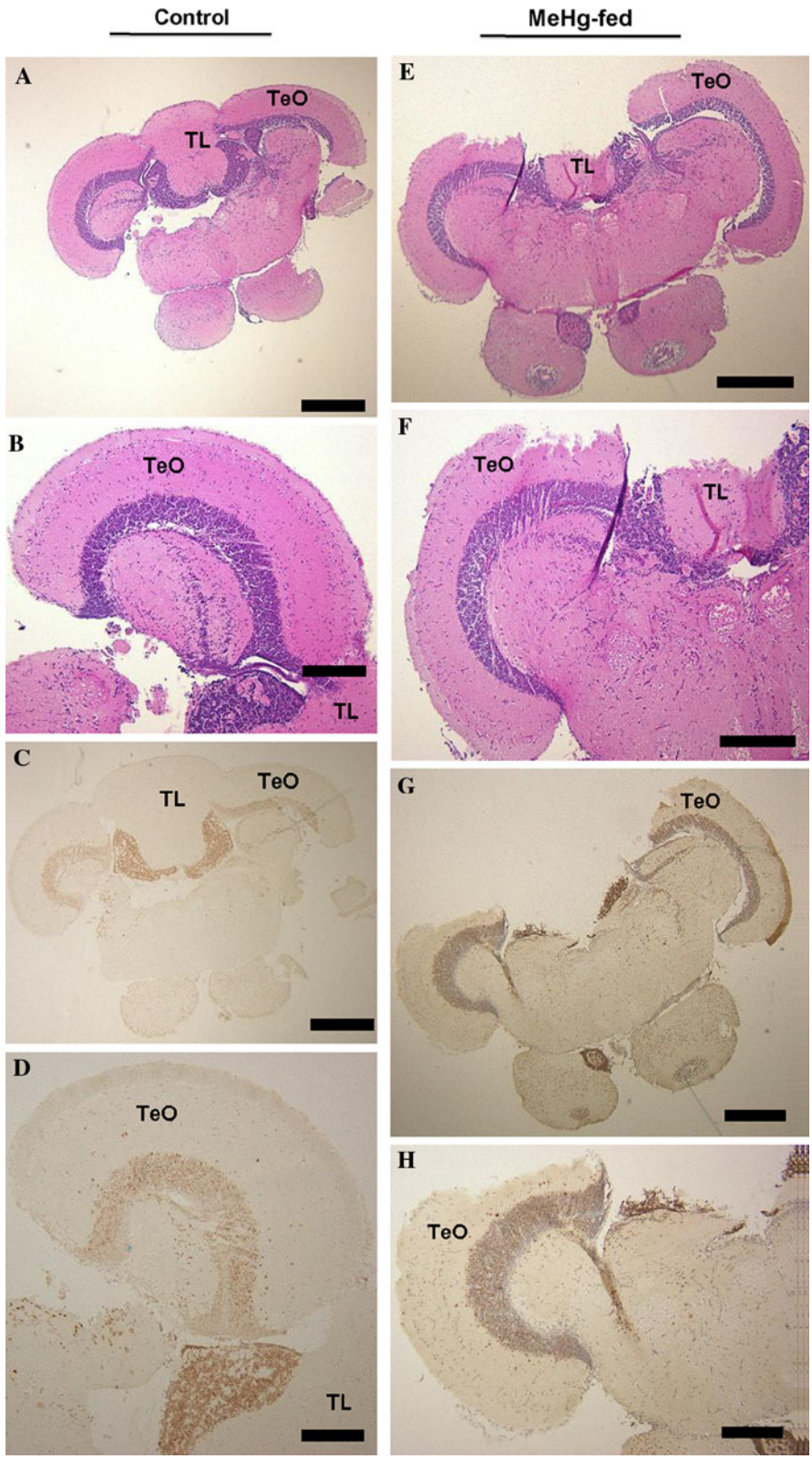
Control
MeHg-fed
A
TeO
TL
E
TeO
TL
B
TeO
TL
F
TeO
TL
C
TL
TeO
G
TeO
D
TeO
TL
H
TeO

◀ **Fig. 3** Histological analysis of control (**a**, **b**, **c**, **d**) and MeHg-treated (**e**, **f**, **g**, **h**) (0.6 μg Hg day^{-1} fish^{-1}) zebrafish brains. Photographs shown are the hematoxylin and eosin staining of the optical tectum cross-sections of zebrafish brain (**a**, **b**, **e**, **f**) and immunohistochemical analyses with an anti-NeuN antibody (**c**, **d**, **g**, **h**). The *scale bars* represent 200 μm in (**a**, **c**, **e**, and **f**), and 100 μm in (**b**, **d**, **g**, and **h**). *TL* Taurus longitudinalis, *TeO* optical tectum

a sensitive and early biomarker of neurotoxicity (O'Callaghan and Sriram 2005). Compatible with this, microscopic analysis of the brains revealed impacts of MeHg on granular cells located in the optic tectum. These impacts were a decrease in cell density and nuclear area in the contaminated group, the latter perhaps reflecting a condensation of the chromatin, a phenomenon already observed in a

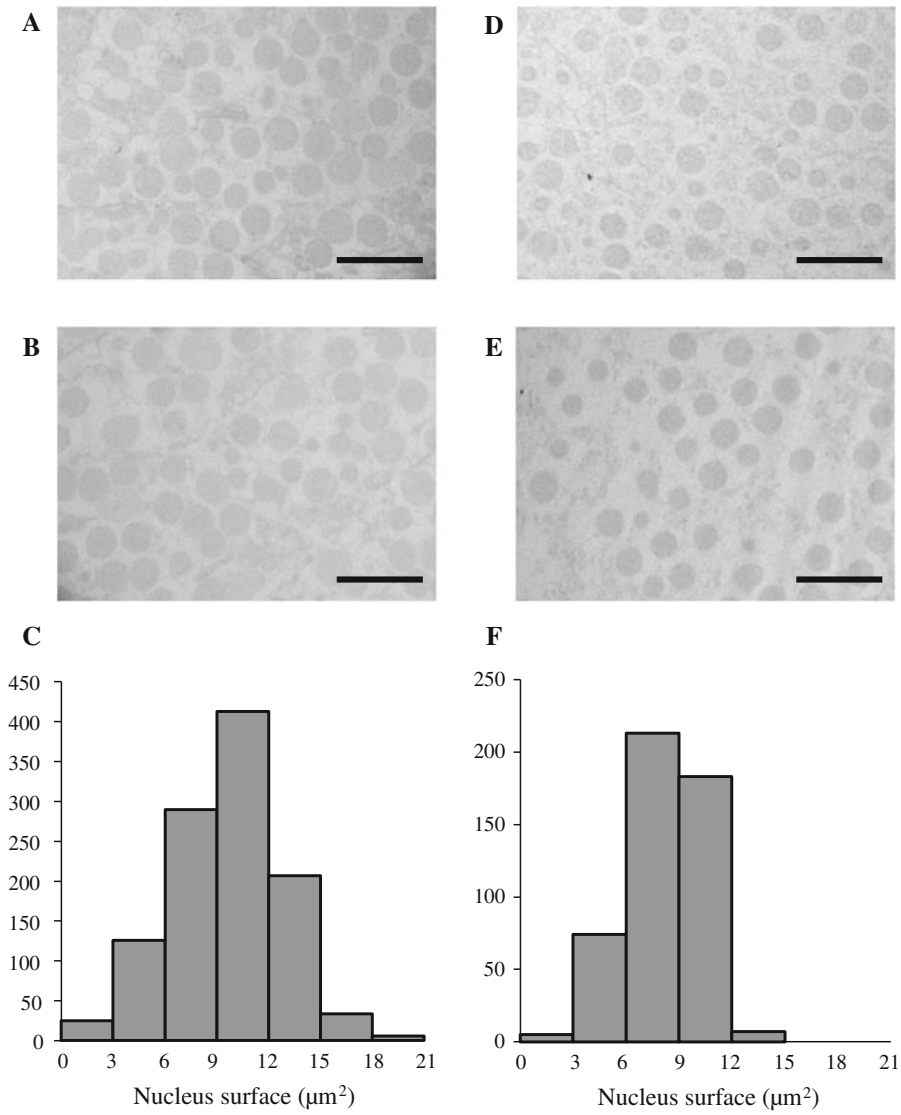

Fig. 4 Impact of methylmercury on *D. rerio* brain after 50 days of dietary exposure to MeHg (0.6 μg Hg day^{-1} fish^{-1}). Shown are cross-sections of granular cells from the optic tectum of control (**a**, **b**) and MeHg-exposed fish (**d**, **e**) (*scale bars* 10 μm). The histograms resulting from image analysis in granular cells and show an impact on the distribution of nucleal surfaces between the 1101 cells counted on the control sections (10 sections per fish from 5 fish) (**c**) and the 482 cells counted on the contaminated sections (6 sections per fish from 4 fish) (**f**) groups

previous study done on human cell cultures exposed to mercuric acetate (Farkas et al. 2010).

Disruption of Ca^{2+} concentration is an early step in MeHg neurotoxicity that leads to cell death in rat cerebellar granule neurons (Marty and Atchison 1997). Transcriptional results obtained in this study showed an up-regulation of three genes encoding the calcium transporters PMCA3a, PMCA3b, and NCX2b after 25 days of exposure to MeHg. This is in keeping with the effects of Hg^{2+} contamination in the mussel *Mytilus galloprovincialis*, which increased both PMCA gene transcription and enzyme activity in the digestive gland (Burlando et al. 2004). However, we cannot explain why the *atp2b3a* and *atp2b3b* genes are up regulated at 25 days and down regulated 25 days later.

In the present work, the transcription of 4 genes involved in glutamate sensing, transport and metabolism remained unaffected after 25 and 50 days of exposure in glutamatergic synapses, a surprising results knowing that glutamatergic synapses are highly sensitive to MeHg. For example, on cultured cerebellar cells, MeHg triggered a substantial release of glutamate and a disruption of glutamate transport at a concentration of 6 mg/l (Fonfria et al. 2005). It was also reported that MeHg was preferentially accumulated in astrocytes, triggering glutamate efflux, inhibiting glutamate reuptake and cysteine transport, leading to depletion of the cellular pools of glutamate and glutathione, and promoting the generation of ROS (Aschner et al. 2007). This might well be due to the fact that we performed contamination on adult animals. Indeed, when newborn rats were exposed on post-natal day 14 to MeHg for seven days at a contamination pressure of 5 μg/g/day, the mRNA transcription of NMDA receptor 2 subunit gene NR2A decreased and that of NR2C increased in cerebral cortex and hippocampus. When the contamination started on post-natal day 60, there was no more difference between contaminated and control groups, showing that the younger the animals are, the more sensitive their brain are to MeHg (Liu et al. 2009). Another possibility is the 10-fold lower contamination pressure we have used on zebrafish (0.6 mg MeHg/kg/day).

One gene involved in the GABA metabolism, *abat*, encoding a GABA transaminating enzyme, was up regulated after 50 days of exposure. This does not fit with the observed decrease of the GABA transaminase activity in brain structures of minks fed a MeHg-containing diet (up to 0.27 mg MeHg/kg body mass/day) (Basu et al. 2010), and the down regulation of the gene encoding the GABA-A receptor gamma 2 subunit in female zebrafish brain 96 h after an acute MeHg exposure (0.5 μg MeHg/g body mass through intraperitoneal injection) (Richter et al. 2011). Further experiments will be necessary to see whether the observed up regulation of the *abat* gene in zebrafish brain has a physiological meaning through monitoring of the GABA transaminase activity.

Acknowledgment We thank Lindsay Hislop for correction of the English language.

References

Akagi H, Malm O, Kinjo H, Harada M, Branches FJP, Pfeiffer W, Kato H (1995) Methylmercury pollution in the Amazon, Brazil. Sci Total Environ 175:85–95

Allen JW, Mutkus LA, Aschner M (2001) Methylmercury-mediated inhibition of 3H-aspartate transport in cultured astrocytes is reversed by the antioxidant catalase. Brain Res 902:92–100

Aschner M (1989) Brain, kidney and liver ^{203}Hg-methyl mercury uptake in the rat: relationship to the neutral amino acid carrier. Pharmacol Toxicol 65:17–20

Aschner M, Yao CP, Allen JW, Tan KH (2000) Methylmercury alters glutamate transport in astrocytes. Neurochem Int 37:199–206

Aschner M, Syversen T, Souza DO, Rocha JB, Farina M (2007) Involvement of glutamate and reactive oxygen species in methylmercury neurotoxicity. Braz J Med Biol Res 40:285–291

Atchison WD (2005) Is chemical neurotransmission altered specifically during methylmercury-induced cerebellar dysfunction? Trends Pharmacol Sci 26:549–557

Basu N, Scheuhammer AM, Rouvinen-Watt K, Evans RD, Trudeau VL, Chan LHM (2010) In vitro and whole animal evidence that methylmercury disrupts GABAergic systems in discrete brain regions in captive mink. Comp Biochem Physiol C 151:379–385

Berg K, Puntervoll P, Valdersnes S, Goksøyr A (2010) Responses in the brain proteome of Atlantic cod (*Gadus morhua*) exposed to methylmercury. Aquat Toxicol 100:51–65

Berntssen MHG, Aatland A, Handy RD (2003) Chronic dietary mercury exposure causes oxidative stress, brain lesions, and altered behaviour in Atlantic salmon (*Salmo salar*) parr. Aquat Toxicol 65:55–72

Burlando B, Bonomo M, Capri F, Mancinelli G, Pons G, Viarengo A (2004) Different effects of Hg^{2+} and Cu^{2+} on mussel (*Mytilus galloprovincialis*) plasma membrane Ca^{2+}-ATPase: Hg^{2+} induction of protein expression. Comp Biochem Physiol C 139:201–207

Cambier S, Benard G, Mesmer-Dudons N, Gonzalez P, Rossignol R, Brethes D, Bourdineaud JP (2009) At

environmental doses, dietary methylmercury inhibits mitochondrial energy metabolism in skeletal muscles of the zebra fish (*Danio rerio*). Int J Biochem Cell Biol 41:791–799

Cambier S, Gonzalez P, Durrieu G, Maury-Brachet R, Boudou A, Bourdineaud JP (2010) Serial analysis of gene expression in the skeletal muscles of zebrafish fed with a methylmercury-contaminated diet. Environ Sci Technol 44:469–475

Charleston JS, Body RL, Bolender RP, Mottet NK, Vahter ME, Burbacher TM (1996) Changes in the number of astrocytes and microglia in the thalamus of the monkey *Macaca fascicularis* following long-term subclinical methylmercury exposure. Neurotoxicology 17:127–138

Clarkson TW, Magos L, Myers GJ (2003) The toxicology of mercury—current exposures and clinical manifestations. N Engl J Med 349:1731–1737

Davis LE, Kornfeld M, Mooney HS, Fiedler KJ, Haaland KY, Orrison WW, Cernichiari E, Clarkson TW (1994) Methylmercury poisoning: long-term clinical, radiological, toxicological, and pathological studies of an affected family. Ann Neurol 35:680–688

de Oliveira Ribeiro CA, Mesmer-Dudons N, Gonzalez P, Dominique Y, Bourdineaud JP, Boudou A, Massabuau JC (2008) Effects of dietary methylmercury on zebrafish skeletal muscle fibres. Environ Toxicol Pharmacol 25:304–309

Denny MF, Hare MF, Atchison WD (1993) Methylmercury alters intrasynaptosomal concentrations of endogenous polyvalent cations. Toxicol Appl Pharmacol 122:222–232

Dreiem A, Seegal RF (2007) Methylmercury-induced changes in mitochondrial function in striatal synaptosomes are calcium-dependent and ROS-independent. Neurotoxicology 28:720–726

Dreiem A, Gertz CC, Seegal RF (2005) The effects of methylmercury on mitochondrial function and reactive oxygen species formation in rat striatal synaptosomes are age-dependent. Toxicol Sci 87:156–162

Durrieu G, Maury-Brachet R, Boudou A (2005) Goldmining and mercury contamination of the piscivorous fish *Hoplias aimara* in French Guiana (Amazon basin). Ecotoxicol Environ Saf 60:315–323

Eto K (2000) Minamata disease. Neuropathology 20:S14–S19

Farkas E, Ujvarosi K, Nagy G, Posta J, Banfalvi G (2010) Apoptogenic and necrogenic effects of mercuric acetate on the chromatin structure of K562 human erythroleukemia cells. Toxicol In Vitro 24:267–275

Fonfria E, Vilaro MT, Babot Z, Rodriguez-Farre E, Sunol C (2005) Mercury compounds disrupt neuronal glutamate transport in cultured mouse cerebellar granule cells. J Neurosci Res 79:545–553

Franco JL, Posser T, Dunkley PR, Dickson PW, Mattos JJ, Martins R, Bainy ACD, Marques MR, Dafre AL, Farine M (2009) Methylmercury neurotoxicity is associated with inhibition of the antioxidant enzyme glutathione peroxidase. Free Radic Biol Med 47:449–457

Fujimura M, Usuki F, Sawada M, Takashima A (2009) Methylmercury induces neuropathological changes with tau hyperphosphorylation mainly through the activation of the c-jun-N-terminal kinase pathway in the cerebral cortex, but not in the hippocampus of the mouse brain. Neurotoxicology 30:1000–1007

Gonzalez P, Dominique Y, Massabuau JC, Boudou A, Bourdineaud JP (2005) Comparative effects of dietary methylmercury on gene expression in liver, skeletal muscle, and brain of the zebrafish (*Danio rerio*). Environ Sci Technol 39:3972–3980

Hare MF, Atchison WD (1995a) Nifedipine and tetrodotoxin delay the onset of methylmercury-induced increase in $[Ca^{2+}]_i$ in NG108-15 cells. Toxicol Appl Pharmacol 135:299–307

Hare MF, Atchison WD (1995b) Methylmercury mobilizes Ca^{2+} from intracellular stores sensitive to inositol 1,4,5-trisphosphate in NG108-15 cells. J Pharmacol Exp Ther 272:1016–1023

Hare MF, McGinnis KM, Atchison WD (1993) Methylmercury increases intracellular concentrations of Ca^{2+} and heavy metals in NG108-15 cells. J Pharmacol Exp Ther 266: 1626–1635

Komulainen H, Bondy SC (1987) Increased free intrasynaptosomal Ca^{2+} by neurotoxic organometals: distinctive mechanisms. Toxicol Appl Pharmacol 88:77–86

Liao BK, Deng AN, Chen SC, Chou MY, Hwang PP (2007) Expression and water calcium dependence of calcium transporter isoforms in zebrafish gill mitochondrion-rich cells. BMC Genomics 8:354

Limke TL, Atchison WD (2002) Acute exposure to methylmercury opens the mitochondrial permeability transition pore in rat cerebellar granule cells. Toxicol Appl Pharmacol 178:52–61

Limke TL, Otero-Montanez JK, Atchison WD (2003) Evidence for interactions between intracellular calcium stores during methylmercury-induced intracellular calcium dysregulation in rat cerebellar granule neurons. J Pharmacol Exp Ther 304:949–958

Limke TL, Bearss JJ, Atchison WD (2004a) Methylmercury causes Ca^{2+} dysregulation and neuronal death in rat cerebellar granule cells through an M3 muscarinic receptor-linked pathway. Toxicol Sci 80:60–68

Limke TL, Heidemann SR, Atchison WD (2004b) Disruption of intraneuronal divalent cation regulation by methylmercury: are specific targets involved in altered neuronal development and cytotoxicity in methylmercury poisoning? Neurotoxicology 25:741–760

Liu W, Wang X, Zhang R, Zhou Y (2009) Effects of postnatal exposure to methylmercury on spatial learning and memory and brain NMDA receptor mRNA expression in rats. Toxicol Lett 188:230–235

Livingstone DR (1998) The fate of organic xenobiotics in aquatic ecosystems: quantitative and qualitative differences in biotransformation by invertebrates and fish. Comp Biochem Physiol A 120:43–49

Malm O, Guimarães JRD, Castro MB, Bastos WR, Viana JP, Branches FJP, Silveira EG, Pfeiffer WC (1997) Follow-up of mercury levels in fish, human hair and urine in the Madeira and Tapajós basin, Amazon, Brazil. Water Air Soil Pollut 97:45–51

Marty MS, Atchison WD (1997) Pathways mediating Ca^{2+} entry in rat cerebellar granule cells following in vitro exposure to methyl mercury. Toxicol Appl Pharmacol 147:319–330

Mori F, Tanji K, Wakabayashi K (2000) Widespread calcium deposits, as detected using the alizarin red S technique, in the nervous system of rats treated with dimethyl mercury. Neuropathology 20:210–215

Mori N, Yasutake A, Hirayama K (2007) Comparative study of activities in reactive oxygen species production/defense system in mitochondria of rat brain and liver, and their susceptibility to methylmercury toxicity. Arch Toxicol 81:769–776

O'Callaghan JP, Sriram K (2005) Glial fibrillary acidic protein and related glial proteins as biomarkers of neurotoxicity. Expert Opin Drug Saf 4:433–442

Oyake Y, Tanaka M, Kubo H, Chichibu M (1966) Neuropathological studies on organic mercury poisoning with special reference to the staining and distribution of mercury granules. Shinkei Kenkyu No Shimpo 10:744–750

Park ST, Lim KT, Chung YT, Kim SU (1996) Methylmercury-induced neurotoxicity in cerebral neuron culture is blocked by antioxidants and NMDA receptor antagonists. Neurotoxicology 17:37–45

Richter CA, Garcia-Reyero N, Martynuik C, Knoebl I, Pope M, Wright-Osment MK, Denslow ND, Tillitt DE (2011) Gene expression changes in female zebrafish (*Danio rerio*) brain in response to acute exposure to methylmercury. Environ Toxicol Chem 30:301–308

Sarafian TA (1993) Methyl mercury increases intracellular Ca^{2+} and inositol phosphate levels in cultured cerebellar granule neurons. J Neurochem 61:648–657

Timme-Laragy AR, Van Tiem LA, Linney EA, Di Giulio RT (2009) Antioxidant responses and NRF2 in synergistic developmental toxicity of PAHs in zebrafish. Toxicol Sci 109:217–227

Usuki F, Yasutake A, Matsumoto M, Umehara F, Higuchi I (1998) The effect of methylmercury on skeletal muscle in the rat: a histopathological study. Toxicol Lett 94:227–232

Usuki F, Yamashita A, Fujimura M (2010) Posttranscriptional defects of antioxidant selenoenzymes causes oxidative stress under methylmercury exposure. J Biol Chem 286:6641–6649

Wiener JG, Krabbenhoft DP, Heinz GH, Scheuhammer AM (2003) Ecotoxicology of mercury. In: Hoffman DJ, Rattner BA, Burton GA, Cairns J (eds) Handbook of ecotoxicology. Lewis Publishers, Boca Raton, FL, pp 409–463